Composites Part C: Open Access 11 (2023) 100364

Contents lists available at ScienceDirect

Composites Part C: Open Access

journal homepage: www.elsevier.com/locate/composites-part-c-open-access

Buckling of simply-supported rectangular Double–Double laminates

Erik Kappel[1]

DLR, Institute of Composite Structures and Adaptive Systems, Lilienthalplatz 7, 38108 Braunschweig, Germany

ARTICLE INFO

Keywords:
Composite design
Double–Double
Buckling
Optimization

ABSTRACT

The family of Double–Double (DD) laminates is in focus of the present study. Well established buckling-cases for rectangular plates are examined in this article from a DD perspective. It is shown that the DD conventions allow for beneficial reformulation of the available equations, which leads to drastic simplification. It is demonstrated that the lightest DD laminate can directly be determined for a specified buckling load. Permutation discussions and the corresponding evaluation of thousands of discrete solutions, known for conventional laminates, become obsolete. The developed DD-buckling equations are further examined from an invariant-based perspective using $I_Q = Q_{11}+Q_{22}+Q_{66}+Q_{12}$ which reveals the important role of the $\sqrt[3]{1/I_Q}$ term for minimum-laminate-thickness calculations.

1. Introduction

Composite structures usually face multiple dimensioning load cases. Stress engineers face the task of identifying a compromise stacking sequence, which can sustain all those individual loads. Comprehensive literature is available for the topic of laminate optimization, which is excellently discussed in recent review articles [1,2]. Identifying the best stacking sequence and assuring laminate zone compatibility is still a challenging task.

Minimizing the structural weight is a common goal in laminate design, which is in focus of this article as well. Thus, the thinnest laminate which can sustain a required buckling load limit is denoted as the *'best'* laminate hereafter. DD laminates are candidates to replace today's conventional laminates, as the DD family promises advantageous by simplifying design, manufacturing and optimization. The present article is focused on buckling analysis of simply supported, rectangular DD laminates, to demonstrate how the DD concept leads to simplification.

1.1. Problem statement

The bending properties of composite laminates, made from unidirectionally (UD) reinforced plies, depend on the stacking sequence. Thus, the coefficients $D_{11}, D_{12}, D_{22}, D_{66}$ of the laminate's bending-stiffness matrix $[D]$ play a key-role within buckling-analysis equations. Those D_{ij}-coefficients depend on additional parameters, such as the plies' Engineering constants, the individual ply orientations, the number of plies in the laminate and the position and order of the individual plies within the whole stack. Engineers need to reduce the design space in order to handle millions of conceivable permutations. In aerospace practice, ply orientations are often limited to the group of (0°, 45°, −45°, 90°) plies. This family is denoted as QUAD hereafter, which is in line with the related literature on Double–Double (DD) laminates later discussed. For QUAD laminates symmetry is usually required to eliminate unwanted coupling effects.[2]

The simple case of a symmetric, quasi-isotropic (QI) laminate is used hereafter to briefly outline the challenge related to permutations. In a QI laminate, composed of (0°, 45°, −45°, 90°) plies, the specific ply-orientation fractions are identical (25%, 25%, 25%, 25%). Conceivable laminate thicknesses are $n \cdot 8 \cdot t_{ply}$. The thinnest laminate in this group has eight plies ($n = 1$). Due to the symmetry constraint one finds $4! = 24$ conceivable stacking sequences. The next thicker laminate in the group has 16 plies ($n = 2$) with $4!^2 = 576$ conceivable stackings. A 32-ply laminate ($n = 4$) already leads to $4!^4 = 331776$ conceivable stackings within the focused laminate family. An easy and elegant procedure for determining the best QUAD laminate does not exist, in particular when multiple adjacent laminate zones need to be compatible.

Within the present article it is demonstrated how the particular laminate architecture of the hereafter introduced family of Double–Double laminates leads to drastic simplifications for the process of determining the 'best' laminate for buckling-relevant load case.

E-mail address: erik.kappel@dlr.de.

[1] As the sole author Erik Kappel is responsible for the whole content.

[2] Additional so called 'stacking-rules' are pursued in practice which are not further discussed here for conciseness.

https://doi.org/10.1016/j.jcomc.2023.100364
Received 16 February 2023; Received in revised form 17 May 2023; Accepted 17 May 2023
Available online 29 May 2023

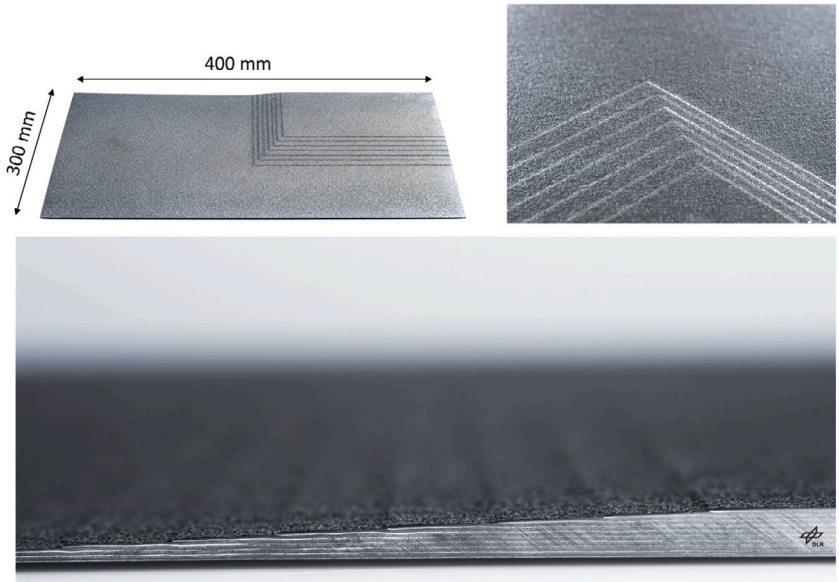

Fig. 1. Locally thickened DD panel with varying BB repeats from $r = 3$ to $r = 10$ and 1:10, 1:20 ramps, which demonstrates how DD promotes patch design.

1.2. Double–Double family of laminates

Double–Double (DD) laminates have been proposed as a promising alternative to conventional, stacking-rule-conform QUAD laminates [3–5]. A DD laminate consists of balanced four-ply building blocks (BB), for example $[\pm\varphi, \pm\psi]$, which are repeated r-times to meet structural requirements. Thus, a DD-laminate is written as $[\pm\varphi, \pm\psi]_{rT}$. φ and ψ are individual ply angles and r denotes the number of repeats. The index T denotes 'total', which follows the convention of Nettles [6, p.27] and the aforementioned publications in DD context.

Asymmetric laminates show complex distortions after manufacturing and when laminates are subjected by mechanical and thermal loads. DD laminates are asymmetric, as BBs are simply stacked on each other without considering any symmetry requirement. However, this particular stacking convention leads to the fact that critical coupling terms in the $[B]$ matrix and the $[D]$ matrix diminish proportional to $1/r$ and $1/r^2$, respectively [5]. This effect is denoted as homogenization, as the ABD-matrix population approaches a state known from isotropic materials, in particular $[B] \rightarrow [0]$ and $D_{16}, D_{26} \rightarrow 0$. Manufacturing-induced distortions, as warping or twist, as well as coupling-driven distortions under mechanical loads diminish as a consequence, even though the DD laminate is asymmetric (See chapter 3 in [4]).

The laminate architecture of the DD-concept promotes local-patch applications, as building blocks can be added locally without the necessity so re-shuffle plies, to keep symmetry or to reconsider the laminate stacking sequences in the adjacent zones.

This creates an independence of the individual laminate zones. Those differ only in the number of BB repeats in a DD laminates. Thus, optimization simplifies to finding the best two ply angles for the BB and the local number of repeats. Stacking-sequence discussions diminish.

While in QUAD laminates, drop-offs of single plies are usually distributed within the laminate stack in through-thickness direction (denoted as staggering), the DD concept features full BB drop-offs (four plies at once). Those BB drop-offs can be located on the parts' outer surfaces preferably, as this helps to avoid laminate-internal resin pockets [7].[3]

Fig. 1 shows a DD-panel example, with a local thickening from $r = 3$ (12 plies) to $r = 10$ (40 plies, 5 mm) [4] repeats. Drop-offs are located on the bag-side surface of the part, which creates a resin-pocket free inner laminate architecture and a minimum out-of-plane ply undulation (see bottom picture in Fig. 1).

Hereafter it is outlined how the unique DD laminate architecture simplifies design for laminates prone to buckling. The process of determining minimum-weight laminates for a given load case is demonstrated.

1.3. DD key basics

Classical laminate theory (CLT) is usually used in composite design [6,8–12]. A normalized formulation is used in context of DD by Tsai and Melo [7, p.164], which can be deduced from CLT.

$$\underbrace{\begin{pmatrix}\{N\}\\ \{M\}\end{pmatrix} = \begin{bmatrix}[A] & [B]\\ [B] & [D]\end{bmatrix} \cdot \begin{pmatrix}\{\varepsilon^0\}\\ \{\varkappa\}\end{pmatrix}}_{\text{CLT}}$$
$$\rightarrow \underbrace{\begin{pmatrix}\{\sigma^0\}\\ \{\sigma^f\}\end{pmatrix} = \begin{bmatrix}[A^*] & [B^*]\\ 3[B^*] & [D^*]\end{bmatrix} \cdot \begin{pmatrix}\{\varepsilon^0\}\\ \{\varepsilon^f\}\end{pmatrix}}_{\text{Normalized}}. \tag{1}$$

Therein, the normalized matrices are defined as

$$[A^*] = \frac{1}{t_{lam}} \cdot [A] \quad , \quad [B^*] = \frac{2}{t_{lam}^2} \cdot [B] \quad , \quad [D^*] = \frac{12}{t_{lam}^3} \cdot [D] \quad , \tag{2}$$

and stresses and strains are $\{\sigma^0\} = \frac{1}{t_{lam}} \cdot \{N\}$, $\{\sigma^f\} = \frac{6}{t_{lam}^2}\{M\}$ and $\{\varepsilon^f\} = \frac{t_{lam}}{2}\{\varkappa\}$. This thickness normalization leads to the fact that all matrices have the same unit of type [Pa]. Hereafter, established buckling relations are examined from the DD perspective, while those equations are updated using the normalized relations presented above.

1.4. Buckling reference scenario

The parametric buckling case of a simply-supported rectangular plate under uni- or bi-axial compression is examined in this article as the reference. It can be found in Reddy [12, p.273] in the utilized parametric form. Fig. 2 shows the scenario, with its parameters.

The critical buckling load for this scenario can be determined using (see Reddy [12, p.273])

$$N_0(m,n) = \frac{D_{11}\alpha^4 + 2\left(D_{12} + 2D_{66}\right)\alpha^2\beta^2 + D_{22}\beta^4}{\alpha^2 + k \cdot \beta^2} \quad \text{with}$$

[3] Laminate-internal drop-offs are conceivable as well. But the effect of larger resin pockets needs further investigation and mechanical tests.

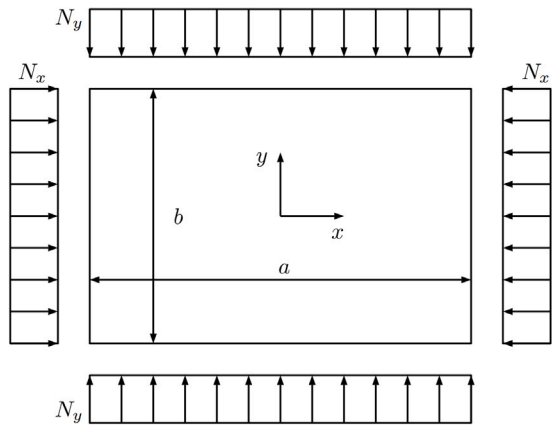

Fig. 2. Scenario in line with Reddy [12, p.273].

$$\alpha = \frac{m\pi}{a},\ \beta = \frac{n\pi}{b},\ k = \frac{N_y}{N_x}$$

m and n denote half waves along x- and y-direction, respectively. Parameters a and b define the panel dimensions. Introducing the terms α, β, k and rearranging leads to

$$N_0(m,n) = \frac{\pi^2}{a^2} \cdot \frac{D_{11}m^4 + 2\left(D_{12} + 2D_{66}\right)m^2n^2\left(\frac{a^2}{b^2}\right) + D_{22}n^4\left(\frac{a^4}{b^4}\right)}{m^2 + k \cdot n^2\left(\frac{a^2}{b^2}\right)} \quad . \tag{3}$$

For a square plate, with ($b = a$), Eq. (3) simplifies to

$$N_0(m,n) = \frac{\pi^2}{a^2} \cdot \frac{D_{11}m^4 + 2\left(D_{12} + 2D_{66}\right)m^2n^2 + D_{22}n^4}{m^2 + k \cdot n^2} \quad . \tag{4}$$

When identical edge-loads are considered ($k = \frac{N_y}{N_x} = 1$) in addition, the relation further simplifies to

$$N_0(m,n) = \frac{\pi^2}{a^2} \cdot \frac{D_{11}m^4 + 2\left(D_{12} + 2D_{66}\right)m^2n^2 + D_{22}n^4}{m^2 + n^2} \quad , \tag{5}$$

which is identical to the demo case in the Milhandbook [13, page 5–75][4]. The D_{ij}-factors in these equations are the $[D]$-matrix coefficients (see Eq. (1)). The D_{ij} are stacking-dependent [13, page 5–77] and determined with $3D_{ij} = \sum_{k=1}^{n}[\bar{Q}]_k(z_k^3 - z_{k-1}^3)$. Numerous discrete stackings must be examined for QUAD to identify the optimum with the corresponding laminate thickness.

The particular architecture of the DD laminate family promises a simplification of the problem. The DD conventions allow for a reformulation of the aforementioned equations, from a $[D]$-based to a $[D^*]$-based formulation. This introduces the important r-parameter, as it is shown hereafter. Based on the thickness-normalized matrix

$$[D^*] = \frac{12}{t_{lam}^3} \cdot [D] = \frac{12}{(r \cdot 4 \cdot t_{ply})^3} \cdot [D] = \frac{3}{16 \cdot t_{ply}^3 \cdot r^3} \cdot [D] \quad , \tag{6}$$

one finds

$$D_{ij} = \frac{16}{3} \cdot t_{ply}^3 \cdot r^3 \cdot D_{ij}^* \quad . \tag{7}$$

Introducing the specific coefficients yields the DD-specific relation

$$N_0(m,n) = \frac{\pi^2}{a^2} \cdot \frac{16 \cdot t_{ply}^3}{3} \cdot r^3 \cdot \frac{D_{11}^*m^4 + 2\left(D_{12}^* + 2D_{66}^*\right)m^2n^2 + D_{22}^*n^4}{m^2 + n^2} \quad . \tag{8}$$

It is worth commenting here that one finds $[A^*] = [D^*]$ for increasing r, while even for small r-values all relevant matrix entries considered in Eq. (8) are equal ($D_{11}^* = A_{11}^*$, $D_{22}^* = A_{22}^*$, $D_{12}^* = A_{12}^*$, $D_{66}^* = A_{66}^*$). Thus, one can rewrite the critical buckling load in terms of $[A^*]$ as

$$N_0(m,n) = \frac{\pi^2}{a^2} \cdot \frac{16 \cdot t_{ply}^3}{3} \cdot r^3 \cdot \frac{A_{11}^*m^4 + 2\left(A_{12}^* + 2A_{66}^*\right)m^2n^2 + A_{22}^*n^4}{m^2 + n^2} \quad . \tag{9}$$

which directly indicate the stacking independence, as $[A^*]$ is stacking independent.

When proceeding from Eq. (8), one can directly solve for r

$$r = \sqrt[3]{N_0(m,n) \cdot \left(\frac{3a^2}{16\pi^2 t_{ply}^3} \cdot \frac{m^2 + n^2}{D_{11}^*m^4 + 2\left(D_{12}^* + 2D_{66}^*\right)m^2n^2 + D_{22}^*n^4}\right)} \tag{10}$$

which leads to the minimum number of BB-repeats that is mandatory to sustain the buckling load N_0. Note, that BB repeats r are proportional to the laminate thickness, as $t_{lam} = 4 \cdot t_{ply} \cdot r$. From Eq. (10), r is usually determined as a float number. Thus, it is important to highlight that r needs to be rounded to the next higher integer value, due to manufacturing convention, saying that the DD laminate concept requires four-ply BBs.

Eq. (10) can be separated in different independent pre-factors and constants. One find a load pre-factor $\sqrt[3]{N_0(m,n)}$, a constant $\sqrt[3]{\frac{3}{16\pi^2}}$, a composite-material-specific pre-factor $\frac{1}{t_{ply}}$ and a plate-dimension pre-factor $\sqrt[3]{a^2}$ (only valid for square plates), as shown hereafter.

$$r = \frac{1}{t_{ply}}\sqrt[3]{N_0(m,n)} \cdot \sqrt[3]{\frac{3}{16\pi^2}} \cdot \sqrt[3]{a^2} \cdot \sqrt[3]{\left(\frac{m^2 + n^2}{D_{11}^*m^4 + 2\left(D_{12}^* + 2D_{66}^*\right)m^2n^2 + D_{22}^*n^4}\right)} \tag{11}$$

All pre-factors neither depend on stacking nor on ply orientations. The last term in Eq. (11) $\sqrt[3]{f(m,n,[D^*])}$ is particularly important. It depends on the ply angles φ and ψ of the BB, the material's Engineering constants (in $[Q]$ used for $[D^*]$) and the buckling form, described by half-waves m and n in x- and y-direction, respectively. It also depends on the panel dimension for non-square ($a \neq b$) configurations.

The minimum r-value refers directly to the minimum laminate thickness required to sustain the considered buckling load. Thus, the minimum r-value relates to the maximum weight-specific buckling resistance of the regarded panel.

$$r \propto \sqrt[3]{\left(\frac{m^2 + n^2}{D_{11}^*m^4 + 2\left(D_{12}^* + 2D_{66}^*\right)m^2n^2 + D_{22}^*n^4}\right)} \tag{12}$$

However, the buckling form is essential. Nine buckling cases are examined hereafter in detail to describe the process of finding the best laminate. Those cases are summarized in Table 1.

Table 1
Buckling cases –m, n denote half waves in x- and y-direction, respectively.

Cases	1	2	3	4	5	6	7	8	9
m	1	1	1	2	2	2	3	3	3
n	1	2	3	1	2	3	1	2	3

All analyses presented hereafter refer to unidirectional IM7/977-3 prepreg material (Data from Tsai [14, p.5]). The relevant Engineering constants and the ply thickness are provided in Table 2.

The corresponding ply-stiffness matrix $[Q]$ and the invariants $I_Q = Q_{11} + Q_{22} + Q_{66} + Q_{12}$ and 'Trace' $Tr = Q_{11} + Q_{22} + 2Q_{66}$ (used later in Section 4) are given by

$$[Q] = \begin{bmatrix} 192.225 & 3.501 & 0 \\ 3.501 & 10.004 & 0 \\ 0 & 0 & 7.790 \end{bmatrix} \text{GPa} \rightarrow \begin{cases} I_Q & = 213.52 \text{ GPa} \\ Tr & = 217.81 \text{ GPa} \end{cases} \quad . \tag{13}$$

[4] Note that Eq. 5.7.1.6(a) is erroneous in the numerator's second term in Milhandbook. $(b/a)^4$ shall be $(b/a)^2$.

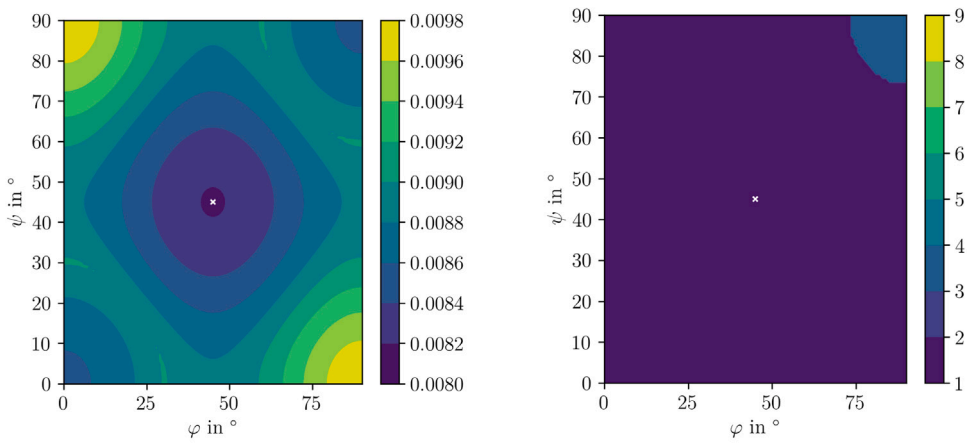

(a) Term in Equation 12 (b) case determining r

Fig. 3. Term from Eq. (12) and dominating $m-n$ case for the maximum r (see Eq. (12)).

Table 2
IM7/977-3 Material data from Tsai [14, p.5].

E_1	191.0 GPa
E_2	9.94 GPa
ν_{12}	0.35
G_{12}	7.79 GPa
t_{ply}	0.125 mm

2. Procedure

The determination process of the best DD-laminate configuration is presented hereafter. A DD laminate can be described by its two independent ply angles φ and ψ in the building block. Thus, simple 2D visualization becomes possible, as demonstrated in laminate optimization context in [5]. Full-degree ply angles are considered hereafter for φ and ψ, which is linked to realistic, feasible manufacturing precision for prepreg ply layup (hand layup and also automated processes such as automated fiber placement (AFP)). Thus, $91^2 = 8281$ ply-angle combinations are considered for all nine half-wave combinations.[5] As the term's magnitude refers to the number of repeats, its minimum leads to the thinnest laminate which can sustain the considered load.

The minimum of all nine half-wave-case-specific calculations is stored for each angle combination φ, ψ, as each minimum refers to the laminate with the highest buckling resistance, which is equivalent to the lowest repeat value.

The square panel case, with identical edge loads ($k = 1$), is further examined hereafter. Fig. 3(a) shows the determined result analysis of the term given in Eq. (12). The global minimum is marked by a white cross, which is found at $\varphi = \psi = 45°$ for the considered square plate.

Fig. 3(b) shows, that half-wave case 1 (see Table 1) is the dominating case for the problem at hand. This is not surprising, as the term (see Eq. (12)) is of kind $x^{-1/3}$, while x is growing rapidly for increasing m and n values. The analysis indicates (see Fig. 3(a)) the particular role of $[\pm 45°, \pm 45°]$ configuration, for which the minimum laminate thickness is needed.

2.1. General formulation

The general form, for rectangular DD-laminate plates ($a \neq b$), subjected to uni- or inhomogeneous bi-axial compression ($k \in \mathbb{R}$), is given by

$$r = \frac{\sqrt[3]{N_0(m,n)}}{t_{ply}} \cdot \sqrt[3]{\frac{3}{16\pi^2}} \cdot \sqrt[3]{a^2} \cdot \sqrt[3]{\frac{m^2 + k \cdot n^2 \left(\frac{a^2}{b^2}\right)}{D_{11}^* m^4 + 2\left(D_{12}^* + 2D_{66}^*\right) m^2 n^2 \left(\frac{a^2}{b^2}\right) + D_{22}^* n^4 \left(\frac{a^4}{b^4}\right)}}. \tag{14}$$

It is used in the following.

3. Application

A square-shaped panel with homogeneous edge loads and a rectangular panel with inhomogeneous edge loads are examined hereafter for sake of verification. Analytic calculations are compared to corresponding finite-element (FE) results, determined with ABAQUS CAE, to verify the propagated direct determination procedure for the 'best' laminate. The FE-model specs are outlined in Appendix.

3.1. Case 1: Square panel, homogeneous edge loads

The square-panel case is defined by the parameters $a = b = 1$ m, $N^{cr} = N_x = N_y = 0.05$ MN/m, $k = N_y/N_x = 1$ and m, n in range $[1, 2, 3]$, $t_{ply} = 0.125$ mm. The parametric Eq. (15)

$$N_0(m,n) = \pi^2 \cdot \frac{D_{11} m^4 \left(\frac{1}{a^4}\right) + 2\left(D_{12} + 2D_{66}\right) m^2 n^2 \left(\frac{1}{a^2 b^2}\right) + D_{22} n^4 \left(\frac{1}{b^4}\right)}{m^2 \left(\frac{1}{a^2}\right) + k \cdot n^2 \left(\frac{1}{b^2}\right)} \tag{15}$$

simplifies for the DD scenario to

$$N_0(m,n) = \frac{\pi^2}{a^2} \cdot \frac{16 \cdot r^3 \cdot t_{ply}^3}{3} \cdot \frac{D_{11}^* m^4 + 2\left(D_{12}^* + 2D_{66}^*\right) m^2 n^2 + D_{22}^* n^4}{m^2 + n^2} \tag{16}$$

and solving for r yields

$$r = \sqrt[3]{N_0(m,n) \cdot \frac{3a^2}{16\pi^2 t_{ply}^3} \cdot \left(\frac{m^2 + n^2}{D_{11}^* m^4 + 2\left(D_{12}^* + 2D_{66}^*\right) m^2 n^2 + D_{22}^* n^4}\right)}. \tag{17}$$

Inserting the parameters from above yields

$$\begin{aligned} r &= 36.84 \sqrt[3]{\frac{N}{m}} \cdot 2134.6 \sqrt[3]{\frac{1}{m}} \cdot \sqrt[3]{\frac{m^2}{N}} \sqrt[3]{f([D^*], m, n)} \\ &= 78638.6 \cdot \sqrt[3]{f([D^*], m, n)} \quad . \end{aligned} \tag{18}$$

[5] Further reduction is possible due to plot symmetry, but not mandatory calculation times of seconds are short already.

Table 3
Particular solutions: red-dot, green-dot and the [45, −45, 45, −45] case.

DD layup	$[D^*]$ in N/mm^2	$\sqrt[3]{f([D^*],1,1)}$	Result
$[D^*_{[45,-45,45,-45]}]$ 'best case'	$\begin{bmatrix} 60098.0 & 44518.0 & 0.0 \\ 44518.0 & 60098.0 & 0.0 \\ 0.0 & 0.0 & 48806.6 \end{bmatrix}$	1.704E−4	r = 13.40, 14 repeats needed, 56 plies
$[D^*_{[10,-10,40,-40]}]$ 'red dot case'	$\begin{bmatrix} 129544.4 & 25790.3 & -8667.8 \\ 25790.3 & 28107.0 & -13294.0 \\ -8667.8 & -13294.0 & 30078.9 \end{bmatrix}$	1.824E−4	r = 14.34, 15 repeats needed, 60 plies
$[D^*_{[30,-30,40,-40]}]$ 'green dot case'	$\begin{bmatrix} 96531.8 & 38772.5 & 2000.7 \\ 38772.5 & 35155.1 & -6059.1 \\ 2000.7 & -6059.1 & 43061.2 \end{bmatrix}$	1.737E−4	r = 13.66, 14 repeats needed, 56 plies

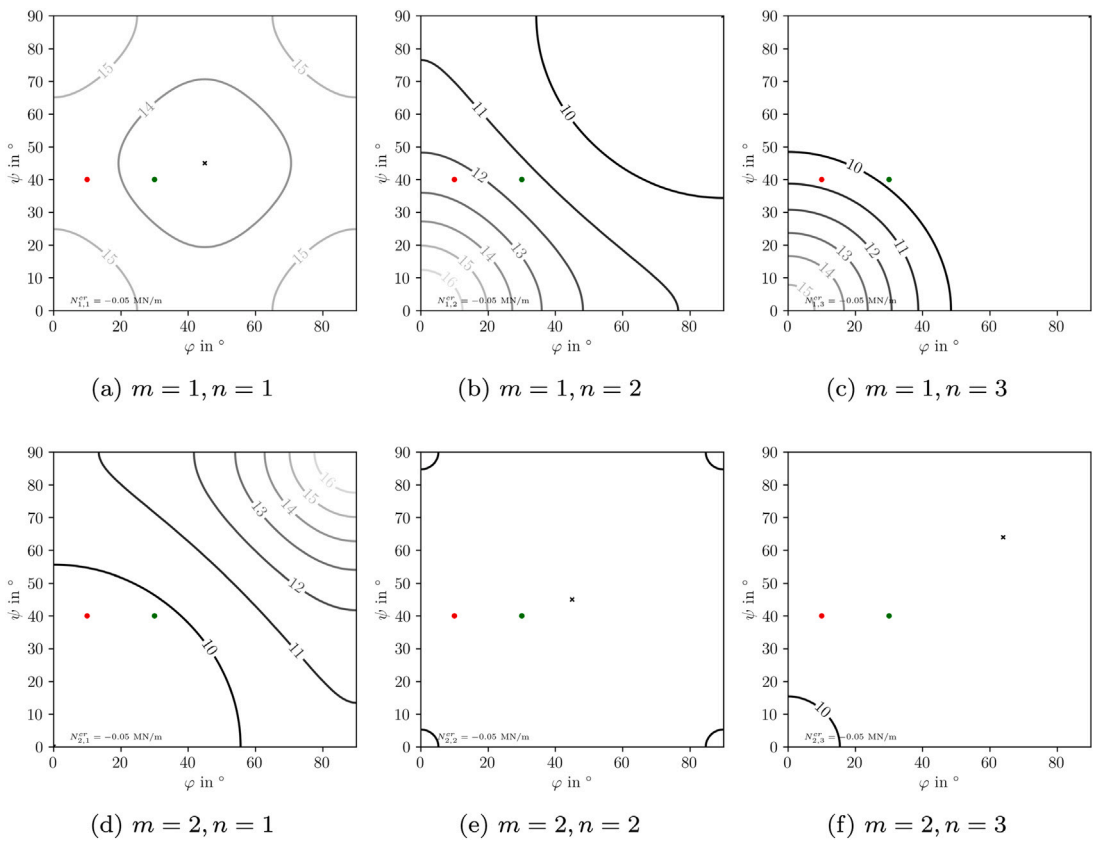

Fig. 4. Minimum number of repeats in DD to sustain the regarded bi-axial compression load. The highest minimum needs to be considered for the laminate. Thus, r = 14 is determined, leading to a 56-ply laminate, with 7 mm thickness.

Fig. 4 visualizes results of the evaluation graphically. For sake of clarity it is focuses on the first six half-wave cases defined in Table 1. Both the red-dot and the green-dot are particular solutions, which are used hereafter to demonstrate the plots' application.

Table 3 lists data for three discrete DD configurations to evaluate the $\sqrt[3]{f([D^*],m,n)}$ term. r is usually determined in $\in \mathbb{R}$ with Eq. (17). However, a manufactured DD laminate shall only feature full BBs per definition. Therefore, above plots show iso-lines, which refer to those integer values. Each plot shows a buckling-case (m,n combination) specific minimum number of repeats. Thus, the highest of those minima determines the minimum laminate thickness. The evaluation of the best case and the green-dot case leads to r-values of 13.xx. Both need to be rounded up to 14, which is the next higher BB count. The red-dot laminate requires r = 15 to sustain the load, as the dot-position is located between 14 and 15 in Fig. 4(a).

Fig. 5 summarizes the result of the preceding analysis. For the case at hand a group of laminates, all with 14 repeats (56 plies), can sustain the load, which is illustrated by the green area. From a weight perspective, all those laminates are equally good. The Margin of safety

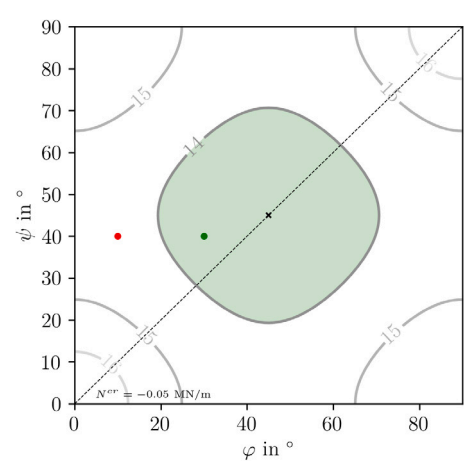

Fig. 5. Feasible region (green area) for minimum-weight laminates with 14 repeats (56 plies, t_{lam} = 7 mm).

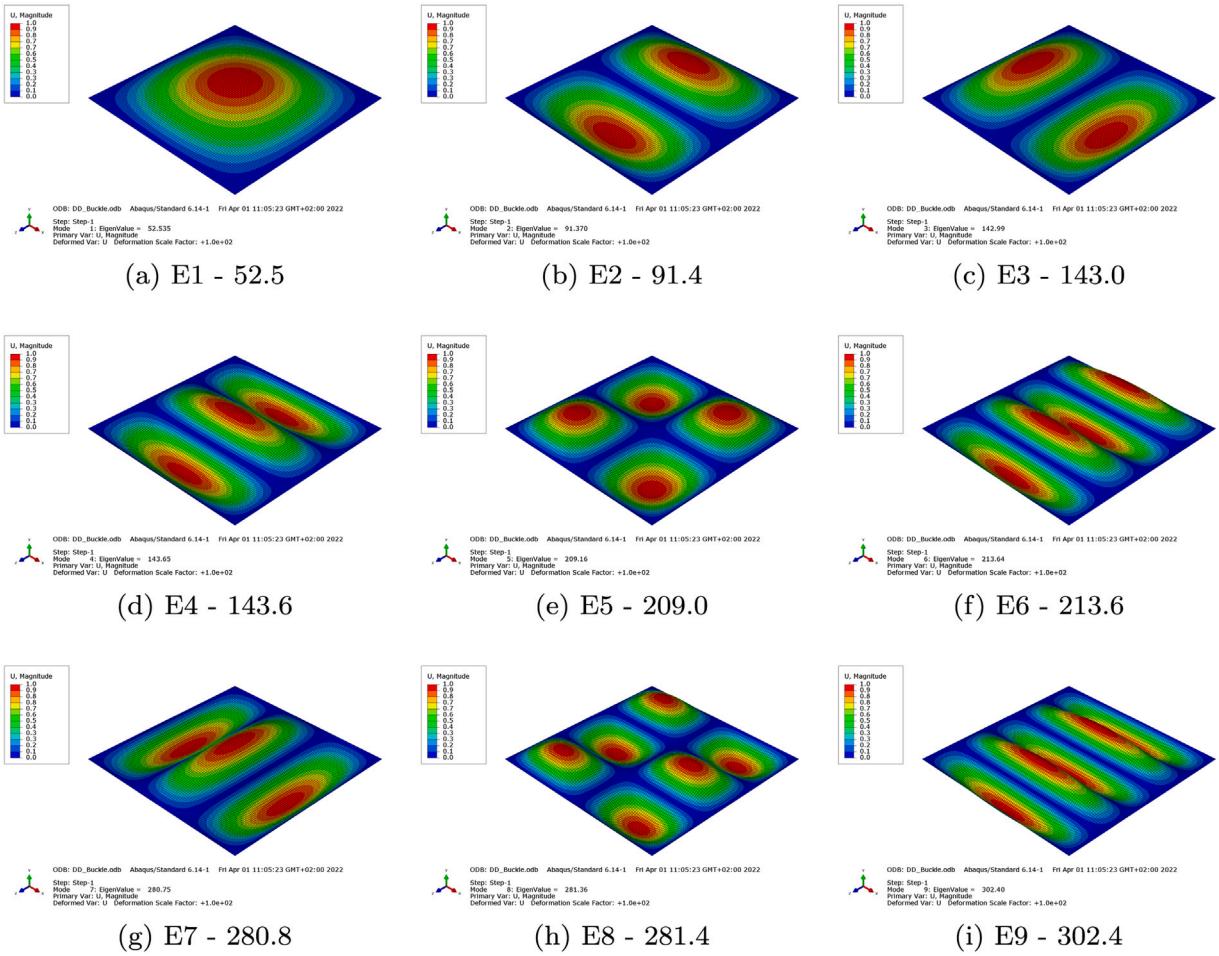

Fig. 6. Eigenvalues for $[\pm 30°, \pm 40°]_{14T}$ laminate is ascending order. Title-block and legend information can be scaled up in the pdf version of the article.

Table 4
Buckling cases $-m$, n denote half waves in x- and y-direction, respectively.

m	1	1	2	1	2	1	3	2	1
n	1	2	1	3	2	4	1	3	5
N_{cr} in MN/m	0.054	0.094	0.146	0.146	0.215	0.217	0.285	0.290	0.307

will be smaller for laminates close to the outer boundary of that area. The determined range allows designers to select from the group of lightest laminates, while the best stacking within the group can be selected based on stiffness requirements, for example (see [5]).

Numerical validation

An Eigenvalue analysis has been performed in ABAQUS to verify the preceding analytic results. The validated modelling procedure, presented in [15], has been adopted for the FE models presented hereafter. An example input file is provided in Appendix. Fig. 6 shows the first nine Eigenvalues for the $[\pm 30°, \pm 40°]_{14T}$ square-plate configuration, which represents the green-dot case from above. The given quantities denoted Ei in the plots refer to compressive edge loads in kN/m.

Table 4 lists the determined critical buckling loads for the buckling configurations in Fig. 6.

The results verify, that for $[30, -30, 40, -40]_{14T}$ (green-dot case) the buckling load of 0.05 MN/m can be sustained by the 56-ply laminate ($14 \cdot 4$, with $t_{lam} = 7$ mm). The discrepancy to the exact value, refers to the up-rounding procedure.

3.2. Case 2: Rectangular panel, deviating edge loads

For a rectangular plate, with the parameters $a = 3b = 3$ m, $N^{cr} = N_x = 0.05$ MN/m, $k = N_y/N_x = 3$, m in range $[1, 2, 3]$, n in range $[1, 2]$, $t_{ply} = 0.125$ mm Eq. (14) leads to

$$r = \sqrt[3]{N_0(m,n) \cdot \left(\frac{3}{16 t_{ply}^3} \cdot \frac{9}{\pi^2} \cdot \frac{m^2 + 27 \cdot n^2}{D_{11}^* m^4 + 2\left(D_{12}^* + 2D_{66}^*\right) m^2 n^2 \cdot (9) + D_{22}^* n^4 \cdot (81)} \right)}. \tag{19}$$

Fig. 7 shows the corresponding case-specific minimum repeats.

Fig. 7a indicates the dominance of the $m = n = 1$ buckling scenario for this load case as well. Only the 20-repeat regions show an overlay for the $m = n = 1$ and the $m = 2$, $n = 1$ region. The determined minimum laminate thickness is 10.0 mm for the material at hand ($4 \cdot 20 \cdot 0.125$ mm) (upper right corner of $m = n = 1$ case). The overlay between $m = n = 1$ and $m = 2, n = 1$ case indicates two very similar buckling loads for the two different half-wave combinations. The corresponding numerical analyses substantiate this observation, as shown in Fig. 8.

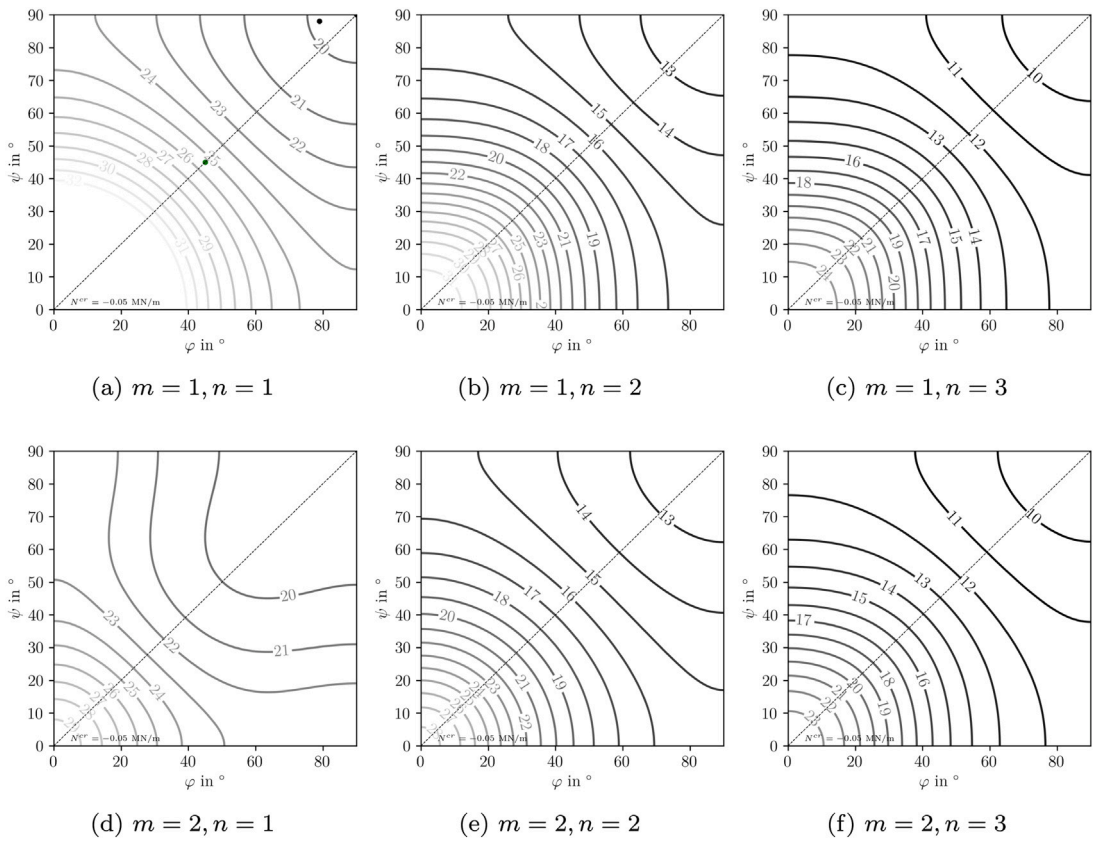

(a) $m = 1, n = 1$ (b) $m = 1, n = 2$ (c) $m = 1, n = 3$

(d) $m = 2, n = 1$ (e) $m = 2, n = 2$ (f) $m = 2, n = 3$

Fig. 7. Minimum number of repeats in DD to sustain bi-axial compressive loads, depending on the DD BB selection. The highest minimum needs to be considered for a certain BB setup.

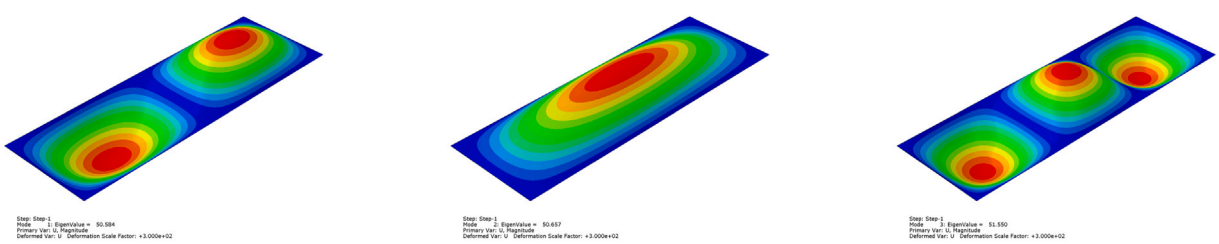

(a) E1 - 50.58 - 2/1 (b) E2 -50.66 - 2/1 (c) E3 - 51.55 - 3/1

Fig. 8. Minimum weight panels with $[\pm 79, \pm 88]_{20T}$ (80 ply, 10 mm laminate thickness)

Fig. 8 shows the first three Eigenvalues of the corresponding case. Two eigenvalues are found very close to each other at 50.58 and 50.66 kN/m, which refer to the two buckling shapes ($m = 2, n = 1$) and ($m = 1, n = 1$), respectively. The numerical minimum is determined for the $[\pm 79, \pm 88]$ BB. The corresponding $[D^*]$ matrix is

$$[D^*_{[\pm 79, \pm 88]}] = \begin{bmatrix} 10454.188 & 6479.049 & 2.340 \\ 6479.049 & 185819.594 & 23.700 \\ 2.340 & 23.700 & 10767.728 \end{bmatrix} \text{MPa} \quad . \tag{20}$$

The analysis of the $\sqrt[3]{f([D^*], m, n)}$ term shows the reason for the very similar r-values, for both m-n states.

for $m = 1, n = 1$:

$$\sqrt[3]{\frac{28}{10454.188 + 18(6479.049 + 2 \cdot 10767.728) + 81 \cdot 185819.594}}$$
$$\sqrt[3]{\frac{28}{81 \cdot 185819.594 \cdot (1 + 0.001 + 0.033)}}$$
$$= 0.01216$$

for $m = 2, n = 1$:

$$\sqrt[3]{\frac{31}{16 \cdot 10454.188 + 72(6479.049 + 2 \cdot 10767.728) + 81 \cdot 185819.594}}$$
$$\sqrt[3]{\frac{31}{81 \cdot 185819.594 \cdot (1 + 0.011 + 0.134)}}$$
$$= 0.01216$$

When for some reason the $[\pm 45, \pm 45]$ optimum laminate from the square-panel case shall be used for the rectangular plate as well, Fig. 7 (green dot) shows that the ($m = n = 1$) case is dominating for this layup. 26 repeats are needed to sustain the defined load case (green dot between the $r = 25$ and the $r = 26$ iso-line) with the selected layup. The corresponding Eigenvalue analysis (see Fig. 9) substantiates the result, with a determined buckling load of 0.0527 MN/m.

A minimum laminate thickness of 13.0 mm (104 plies) is needed to sustain the defined load with the prescribed laminate configuration. This is a 30% penalty compared to the optimum 80-ply laminate (see Fig. 8), determined before.

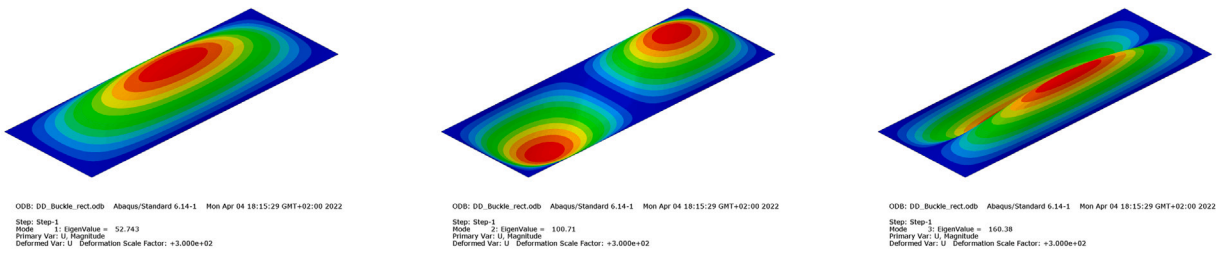

(a) E1 - 52.7 - 1/1 (b) E2 - 100.7 - 2/1 (c) E3 - 160.4 - 1/2

Fig. 9. Eigenvalues (first three) for the $[\pm 45°, \pm 45°]_{26T}$ laminate. The given Eigenvalues refer to buckling load in kN/m (not MN/m).

4. An invariant-based perspective on DD buckling

Invariants of the plies' stiffness matrix $[Q]$ are frequently used in composite design [7,16,17]. The so-called 'Trace' has been proposed by Tsai, Melo and co-workers as a basis to generalize design processes. It is defined as $Tr = Q_{11} + Q_{22} + 2Q_{66}$. In a recent publication [18] it is shown that known invariants of $[Q]$ are all covered by a parametric equation. A new invariant I_Q was found particularly practical, as it is simply defined as the sum of all individual $[Q]$-matrix coefficients $I_Q = Q_{11} + Q_{22} + Q_{12} + Q_{66}$. Both, T_r and I_Q can be considered materials constants (see [14]). The idea of using invariant-based approaches is to generalize analyses for a whole group of similar materials, as for example unidirectionally reinforced carbon-fibre-epoxy-resin laminates. The material-specific invariant is used at the end of the generalized analysis process to transfer the general solution towards a material-specific solution. The invariant I_Q is used hereafter to outline an invariant-focused perspective on the previous buckling cases. I_Q is used as a scalar pre-factor in $[Q]$.

$$[Q] = I_Q \cdot [Q^{I_Q}], \quad \text{(equivalent for 'trace'}[Q] = Tr \cdot [Q^{Tr}]) \tag{21}$$

Note, that $Q_{11}^{I_Q} + Q_{22}^{I_Q} + Q_{66}^{I_Q} + Q_{12}^{I_Q} = 1$. As I_Q is invariant from ply rotation, it acts (and Tr as well) as a pre-factor in $[D^*]$ as well.

$$[D^*] = \frac{12}{t_{lam}^3} \cdot \frac{1}{3} \cdot I_Q \cdot \sum_{k=1}^{n} [\bar{Q}^{I_Q}] \left(h_k^3 - h_{k-1}^3\right) \tag{22}$$

Thus, I_Q-specific terms can be introduced in the buckling relation.

Recalling the $[\pm 30, \pm 40]$ case from above, with

$$[D^*_{[30,-30,40,-40]}] = \begin{bmatrix} 96531.8 & 38772.5 & 2000.7 \\ 38772.5 & 35155.1 & -6059.1 \\ 2000.7 & -6059.1 & 43061.2 \end{bmatrix} \text{N/mm}^2 \tag{23}$$

one finds the I_Q-normalized $[D^*]$ matrix as

$$[D^{*,I_Q}_{[30,-30,40,-40]}] = \begin{bmatrix} 0.452 & 0.182 & 0.009 \\ 0.182 & 0.165 & -0.028 \\ 0.009 & -0.028 & 0.202 \end{bmatrix} \quad \text{with} \quad I_Q = 213.52 \text{ GPa}. \tag{24}$$

With $D^*_{ij} = I_Q \cdot D^{*,I_Q}_{ij}$ one can rewrite Eq. (14), leading to

$$r = \frac{\sqrt[3]{N_0(m,n)}}{t_{ply}} \cdot \sqrt[3]{\frac{3}{16\pi^2}} \cdot \sqrt[3]{a^2} \cdot \sqrt[3]{\frac{1}{I_Q}} \cdot \sqrt[3]{\frac{m^2 + k \cdot n^2 \left(\frac{a^2}{b^2}\right)}{D_{11}^{*,I_Q} m^4 + 2\left(D_{12}^{*,I_Q} + 2D_{66}^{*,I_Q}\right) m^2 n^2 \left(\frac{a^2}{b^2}\right) + D_{22}^{*,I_Q} n^4 \left(\frac{a^4}{b^4}\right)}} \quad .$$

It says that r is proportional to the product of two material-dependent factors.

$$r \propto \sqrt[3]{\frac{1}{I_Q}} \cdot \sqrt[3]{\frac{1}{D_{11}^{*,I_Q} m^4 + 2\left(D_{12}^{*,I_Q} + 2D_{66}^{*,I_Q}\right) m^2 n^2 \left(\frac{a^2}{b^2}\right) + D_{22}^{*,I_Q} n^4 \left(\frac{a^4}{b^4}\right)}} \tag{25}$$

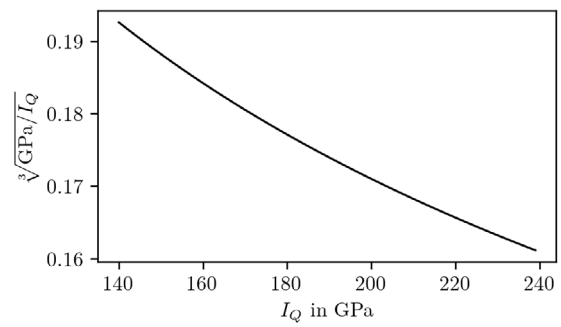

Fig. 10. I_Q-factor magnitude.

Table 5
T700 C-Ply 55 from Tsai [14, p.5].

E_1	121.0 GPa
E_2	8.0 GPa
ν_{12}	0.30
G_{12}	4.7 GPa
t_{ply}	0.125 mm
I_Q	136.9 GPa

With the data from Tsai [14, p.5] one finds a realistic I_Q-range of 150 GPa $\leq I_Q \leq$ 230 GPa. Fig. 10 shows that the I_Q-factor magnitude in Eq. (25) changes only very little for the outlined I_Q range.

For assessing the relevance of $\sqrt[3]{([D^*], m, n)}$ in Eq. (25) a low I_Q material is introduced here (see Table 5) aside from the high I_Q material IM7/977-3 (see Table 2), with $I_Q = 213.52$ GPa.

The $[D^*]$ matrix, of the low-I_Q material is determined to

$$[D^{*,\text{low } I_Q}_{[30,-30,40,-40]}] = \begin{bmatrix} 0.447 & 0.184 & 0 \\ 0.184 & 0.167 & 0 \\ 0 & 0 & 0.201 \end{bmatrix} \quad . \tag{26}$$

Table 6 summarizes the analysis of both factors in Eq. (25), for both materials.

The analysis clearly shows that $\sqrt[3]{\frac{1}{I_Q}}$ is the dominating term in Eq. (25), while the term $\sqrt[3]{([D^*], m, n)}$ has little relevance only. Thus, one can simply transfer the determined results from one to another material by using

$$r_{high,I_Q} \approx \sqrt[3]{\frac{I_{Q,low}}{I_{Q,high}}} \cdot r_{low,I_Q} \quad . \tag{27}$$

Table 6
Evaluation of Eq. (25) for the high and low I_Q material. (...) is the relative difference to High-I_Q material value.

Material	I_Q in GPa	$\sqrt[3]{1/I_Q}$	$\sqrt[3]{([D^*], m, n)}$	$r \propto$
High I_Q	213.52	0.167	1.0481	0.1750
Low I_Q	136.90 (−36%)	0.188 (+12.6%)	1.0446 (−0.3%)	0.1964 (+12.2%)

5. Conclusion

The presented study shows how established equations for buckling problems of simply-supported rectangular plates can be reformulated for the family of DD laminates. It is shown that DD's utilized thickness-normalized description leads to drastic simplification of the buckling relations. The minimum number of building-block repeats (proportional to laminate thickness) can directly be calculated for a specified buckling load and the individual half-wave patterns. Thus, discussions on stacking-sequence optimization, know from the established QUAD laminates, become obsolete for DD.

The presented DD-specific equations are applied for two use cases. A square-shaped panel with homogeneous edge loads ($k = a/b = 1$) and a rectangular panel ($a/b = 3$) with inhomogeneous edge loads ($k = 3$) are examined for sake of verification.

The results of the developed equations are verified by FE-based buckling-load analyses using ABAQUS CAE. Due to the restriction to full-degree ply-orientation angles, which is in line realistic technical manufacturing limits, the best combination for DD's building block angles φ and ψ can be simply identified by picking the best solution out of 91^2 calculations, which takes milliseconds to calculate of a desktop PC.

The developed terms have additionally been transferred to an invariant-based form, to demonstrate how results from one material can be extrapolated to another material. The invariant-based relations feature the invariant $I_Q = Q_{11} + Q_{22} + Q_{12} + Q_{66}$, which has been recently presented by the author. I_Q can be considered a material constant. The study reveals that the minimum DD laminate thickness scales proportional to $r \propto \sqrt[3]{1/I_Q}$. Thus, the effect of substituting a high-I_Q material for a low-I_Q material on the laminate thickness can be quantified by using $r_{high,I_Q} \approx \sqrt[3]{I_{Q,low}/I_{Q,high}} \cdot r_{low,I_Q}$, which can support designers in material selection processes.

Declaration of competing interest

The authors declare that they have no known competing financial interests or personal relationships that could have appeared to influence the work reported in this paper.

Data availability

No data was used for the research described in the article.

Acknowledgments

The research leading to these results has received funding from the German Federal Ministry for Economic affairs and climate action (BMWK) under project number 20A2103C (MuStHaF-DLR).

Appendix. ABAQUS FE-model specs

The used FE model were set up in ABAQUS CAE 6.14. They feature an eigenvalue buckling prediction step, as is described in detail in [15]. The analysis returns Eigenvalues. The predicted buckling load is determined by multiplying a determined eigenvalue with the applied load.

The code hereafter shows the relevant content of the Abaqus input file used in Section 3.2. The model dimensions are in mm, the material is defined in N/mm^2.

Listing 1: ABAQUS input file skeleton

```
*NODE
ADD coordinates here
1, 0.,0.,0
101,3000.0,0.,0.
1617,0.,1000.0,0.
1717,3000.0,1000.0,0.
...

*ELEMENT,TYPE=S4R
1,1,2,103,102
...

*****************************************
*****************************************
*****************************************
*NSET,NSET=BZ
YPAR,XPAR
*NSET,NSET=BX
1,1617
*NSET,NSET=BY
1,101
*****************************************
*Orientation, name=Ori-1
1.,0.,0.,    0.,1.,0.
3, 0.
*Shell Section, elset=PLATE, composite,
    orientation=Ori-1, layup=CompositeLayup-1
0.1250, 3, ply, 30.0, Ply1_r1
0.1250, 3, ply, -30.0, Ply2_r1
0.1250, 3, ply, 40.0, Ply3_r1
0.1250, 3, ply, -40.0, Ply4_r1
...

*****************************************
*Elset, elset=_Surf-2_E4, generate
1,1501,100
*Elset, elset=_Surf-2_E2, generate
100,1600,100
*Surface, type=ELEMENT, name=Surf-x
_Surf-2_E4, E4
_Surf-2_E2, E2
*****************************************
*Elset, elset=_Surf-1_E1, generate
1, 100, 1,
*Elset, elset=_Surf-1_E3, generate
1501 , 1600, 1,
*Surface, type=ELEMENT, name=Surf-y
_Surf-1_E1, E1
_Surf-1_E3, E3
*****************************************
*Material, name=ply
*Elastic, type=LAMINA
191000.,9940., 0.35,7790.,7790.,4500.
*****************************************
*Step, name=Step-1, nlgeom=NO, perturbation
*Buckle
10, , 18, 50
*****************************************
*****************************************
*Boundary, op=NEW, load case=1
BY, 2, 2
*Boundary, op=NEW, load case=2
BY, 2, 2
*Boundary, op=NEW, load case=1
BX, 1, 1
*Boundary, op=NEW, load case=2
BX, 1, 1
*Boundary, op=NEW, load case=1
BZ, 3, 3
*Boundary, op=NEW, load case=2
BZ, 3, 3
*****************************************
*Dsload
Surf-x, EDNOR,1
*Dsload
Surf-y, EDNOR,3
*Restart, write, frequency=0
*Output, field, variable=PRESELECT
*End Step
```

References

[1] S. Nikbakt, S. Kamarian, M. Shakeri, A review on optimization of composite structures part I: Laminated composites, Compos. Struct. 195 (2018) 158–185.
[2] Y. Xu, J. Zhu, Z. Wu, Y. Cao, Y. Zhao, W. Zhang, A review on the design of laminated composite structures: Constant and variable stiffness design and topology optimization, Adv. Compos. Hybrid Mater. 1 (2018) 460–477.
[3] S.W. Tsai, Double-double: New family of composite laminates, AIAA J. (2021) http://dx.doi.org/10.2514/1.J060659.
[4] S.W. Tsai, et al., DOUBLE-DOUBLE A New Perspective in the Manufacture and Design of Composites, JEC/ Stanford publication, ISBN: 978-0-9819143-3-6, 2022.
[5] E. Kappel, Double-double laminates for aerospace applications - Finding best laminates for given load sets, Compos. Part C: Open Access 8 (2022) 100244.

[6] A.T. Nettles, Basic Mechanics of Laminated Composite Plates - NASA Reference Publication 1351, Technical Report, NASA, 1994.
[7] S.W. Tsai, J.D.D. Melo, Composite Materials Design and Testing - Unlocking Mystery with Invariants, Stanford University, 2015.
[8] K. Moser, Faser-Kunststoff-Verbund. Entwurfs- Und Berechnungsgrundlagen, VDI Verlag, 1992.
[9] VEREIN DEUTSCHER INGENIEURE, VDI 2014 Blatt 3 / part 3. Development of FRP components (fibre reinforced plastics) analysis, 2006.
[10] A. Baker, M. Scott, Composite Materials for Aircraft Structures, American Institute of Aeronautics & Astronautics, 2016.
[11] R.M. Jones, Mechanics of Composite Materials, second ed., Taylor & Francis, 1999.
[12] J.N. Reddy, Mechanics of Laminated Composite Plates and Shells, Theory and Analysis, second ed., CRC Press, 2004.
[13] Department of Defense, Composite materials handbook. Polymer matrix composites materials usage, design, and analysis. MIL-HDBK-17-3F, Vol. 3 of 5, 17 June 2002.
[14] S. Tsai, N. Sharma, A. Arteiro, S. Roy, B. Rainsberger, Composite double-double and grid/skin structures a Stanford/Mtorres invention. Low weight/low cost design and manufacturing International Paris Air Show, 2019.
[15] Dassault Systems, Abaqus 6.14 online documentation. Abaqus example problems guide, section: 1.2.2 laminated composite shells: Buckling of a cylindrical panel with a circular hole, 2014.
[16] S.W. Tsai, N.J. Pagano, Invariant Properties of Composite Materials, Technical Report, Air Force Material Laboratory, 1968, AFML-TR-67-349.
[17] S.W. Tsai, J.D.D. Melo, An invariant-based theory of composites, Compos. Sci. Tech. (2014).
[18] E. Kappel, On invariant combinations of Q_{ij} coefficients and a novel invariant I_Q. Composites: Part C open access, 10, 100335, 2023.